Title: Variations in optical power of terrestrial and oceanic lightning as observed by C/NOFS

Authors: Makenna C. Reeves, Robert H. Holzworth, Abram R. Jacobson, Michael P. McCarthy

Abstract

We analyze optical lightning data from the Communications/Navigation Outage Forecasting System (C/NOFS) satellite between April 2008 and March 2011 using the World Wide Lightning Location Network (WWLLN). The Lightning Detector (LD) consists of a pair of photodiodes with a field of view varying by altitude. We briefly describe the instrument and then compare lightning events over ocean and land. We find that there is a greater probability of an optical emission occurring over the ocean to register at a higher peak optical power than an optical emission occurring over the land. That is to say the average optical power for strokes over the ocean is found to be larger than that from land based strokes. Additionally, we find that the high optical power events are statistically associated with areas of lower outgoing longwave radiation fluxes. Comparing land and ocean optical emissions to outgoing longwave radiation fluxes we find that oceanic optical emissions correspond to higher fluxes than those over land.

1. Introduction

Every year thunderstorms and lightning are directly responsible for forest fires, delays in air traffic, disturbances in public utilities, and even death. Lightning has been linked to a wide range of phenomena including severe storm development [Gatlin and Goodman, 2010, Williams et al., 1999]; atmospheric phenomena such as transient luminous events (TLEs) which include sprites and elves [Sabbas et al., 2010, Hsu et al., 2009]; and magnetospheric phenomena including particle loss from the radiation belts [Rodger et al., 2003]. The need for global lightning detection and mapping is essential not only for personal safety but to further study such effects of lightning.

Many methods of lightning detection have been employed as far back as the end of the 19th century. Today we have at our disposal numerous land based lightning networks and arrays such as the World Wide Lightning Location Network (WWLLN) [Lay et al., 2005; Rodger et al. 2006] and National Lightning Detection Network (NLDN) [Abarca et al., 2010]. Additionally, the observation and mapping of global lightning patterns by satellite began in the 1960's. Currently Active detectors in space include instruments on the TRMM and C/NOFS satellites. By 2015 we expect the launch of GOES-R that would provide continuous lightning mapping over the majority of the western hemisphere.

The severity of a thunderstorm has been linked to flash rate, storm height, and the ratio of in cloud versus cloud to ground lightning [MacGorman et al 1989, Ushio et al 2001]. Regional differences in flash rate and cloud height have been discussed by Orville and Henderson [1986], and Price and Rind [1992]. Boccippio et al [2000] has shown that not only does flash rate differ between oceanic and continental cells but that flash radiance differs as well suggesting an underlying geophysical source of land/ocean differences in lightning. Some suggested causes for this difference are cloud optical properties and water content.

Outgoing longwave radiation (OLR) at the top of the atmosphere (TOA) is dependent on cloud top temperatures, optical depth, and water content. This makes OLR a decent proxy for convection [Heddinghause and Krueger, 1981; Waliser et al., 1993; Chen et al, 2000].

In this study, we use three years of satellite optical lightning data from C/NOFs to investigate to power variations over land and ocean, and then we investigate a difference between ocean and land in lightning optical power. Using data gathered over 2008-2011 by C/NOFS and WWLLN, we compare a subset of lightning data with regional outgoing longwave radiation flux measurements (OLR) at the top of the atmosphere. We first verify the lightning detector aboard C/NOFS satellite by comparing the geographic distribution of lightning and optical power to previous studies. We then conduct a preliminary investigation of a possible relationship between lightning and outgoing longwave radiation (OLR) flux.

2. Instrumentation

2.1 Lightning Detector (LD) aboard C/NOFS

In 2008 the Vector Electric Field Investigation (VEFI) aboard the Communications/Navigation Outage Forecasting System (C/NOFS) satellite was launched into a near-equatorial orbit. Its instrumentation includes an optical Lightning Detector (LD) that identifies optical events. This LD continuously observes lightning during nighttime passes of the satellite along its low inclination (13 degree) orbit and within the altitude domain defined by the satellite's perigee and apogee of 401 km and 867 km, respectively. The LD gathers data within 15-30 degrees latitude of the subtrack and records optical intensity in seven discrete power levels from a pair of photodiode detectors (one north looking, the other south looking) each with an inner and outer field of view (FOV). In this study we will only use data from the inner FOV.

A detailed description of the LD instrument and FOV has been given by Jacobson et al. [2011]. We therefore include only a summarized description of the data acquisition methodology. To estimate optical emissions, the LD instrument operates in a low-rate acquisition mode and samples incident light every half second. A 12-bit digitizer samples an amplified analog photodiode signal at 8 kHz and converts the resulting samples to counts which are then binned according to optical power into seven discrete power bins. These bins are referred to in this paper as LD0 through LD6. That is, during each ½ second the number of 0.124 millisecond samples (taken at 8 kHz rate) during which the optical power was within the bands are accumulated in the bins LD0 thought LD6.

2.2 World Wide Lightning Location Network

The World Wide Lightning Location Network (WWLLN) provides real-time locations of lightning strokes using VLF receivers from approximately 50 stations around the world during the time period of this study. By requiring each stroke to be detected by at least 5-stations, WWLLN provides an accuracy of stroke location to within approximately 10 km [Rodger et al., 2005]. The detection capability for stroke events by WWLLN is limited by its asymmetric detection efficiency. While WWLLN can detect both cloud-to-ground (CG) strokes and intra-cloud (IC) strokes, the CG strokes tend to have greater peak current and therefore higher detection efficiency [Lay et al. 2004, Rodger et al., 2005]. At the time of this study, the overall detection efficiency (DE) of WWLLN was approximately 10% [Abarca et al., 2010].

We choose to use WWLLN for this experiment, despite a relatively low DE because WWLLN provides global coverage whereas regional network detections are limited to within a few hundred kilometers of the coast with little coverage in the C/NOFS path.

2.3 Outgoing Longwave Radiation (OLR) flux

The outgoing longwave radiation (OLR) flux data used for this study are from the NOAA/ERSL PSD data [Mesinger, Fedor et al., 2004] set where OLR values are determined from the hourly mean. The area of interest is roughly bounded by -180° to -40° in longitude and from the equator to 40°N in latitude.

3. Methodology

In this study we only sample data where the LD instrument is in eclipse (i.e. in the Earth's shadow). Each eclipse pass consists of roughly 2000 seconds or approximately 4000 half-second LD reports. We define a lightning event as a given ½ second when the LD is triggered. Each event is then assigned to an LD-level defined to be the highest power bin triggered in that half-second.

We use the World Wide Lightning Location Network (WWLLN) as a ground truth and to locate candidate strokes for each LD event. Candidate strokes are defined to be all strokes within the instantaneous inner field of view (FOV) (Jacobson et al., 2011). We define candidate strokes as the subset of strokes that occur within the ½ second collection period when inner FOV of the LD detects an event. We discard events if more than one WWLLN stroke is detected during this ½ second collection period. This is because the LD is non-imaging and cannot on its own determine the location of an event within its FOV. From here on out we will refer to all events detected by the LD as LD-events whereas the subset of LD-events and their respective strokes as events with stroke location.

4. Results and Discussion

Over the time period November 2008 through October 2011 the LD observed 790,730 events whereas WWLLN detected 1,757,118 candidate strokes in the LD FOV. The total number of coincident LD events and WWLLN strokes (event/stroke pairs) detected was 20,789. We amassed this subset into 5-degree bins between +/- 35 degrees in latitude and +/- 180 degrees in longitude.

To verify that the LD only observed events during nighttime the time for each event with stroke location was binned by hourly increments of local time. We found that the events peak at 2000 local time and that no events were detected between the daylight hours of 0700 and 1700 local time [Figure 1]. A previous study done by Lay et al. [2007] found the peak for land lightning to occur in the afternoon to evening hours with a near continuous background level of oceanic lightning. As the LD is restricted to exclusively nighttime hours, we see here the tail end of the land peak and a background level of ocean lightning before the dawn cut-off.

We first address possible sources of count bias due to signal attenuation. Due to altitude variations of the satellite, the apparent LD-level of a given event pair may be falsely assigned to a lower energy bin relative to an event observed from a lower-altitude orbit. We therefore correct the apparent LD-level for altitude as follows. We utilize WWLLN to locate the source stroke for each LD event and normalize

the optical power to the ideal distance of a stroke occurring directly under the satellite at perigee, or 400 km. Using the distance between the sub-satellite point, the location of each relevant stroke, and the altitude of the satellite during detection, we calculate the distance between each stroke and the satellite. We define a rule for applying an event LD-level bin correction by first determining the midpoint value of the bin to estimate the minimum distance between a candidate stroke and the LD required to assign each event into the adjacent, higher power bin. We compare the minimum distance required for this power bin correction to the distance to the LD and adjust the LD-level accordingly. In many cases the power bin of an event is advanced up by more than 1 LD-level. We find that without any altitude correction the events were significantly biased toward LD 0. After the altitude correction was performed the event/stroke pairs distributed differently through the LD-levels (Table 1).

4.1 Comparison of WWLLN and C/NOFS

We compare the distribution events detected by the LD to those coincidentally located by WWLLN. We first plot all LD events in 5-degree bins of longitude. The sub-satellite point is used for the location of the event. Similarly, the events that are coincidentally located by WWLLN are also plotted in 5-degree bins by the longitude of the location of the stroke (Figure 2). It is clear that the LD is capable of detecting optical lightning emissions across all longitudes.

The relative decrease of the lower plot over Africa (20 long) is interesting. When looking at all LD events (top panel), the regions with the most events are Europe/Africa then followed by the maritime continent and Americas respectively. However, when WWLLN is used to locate the source stroke for events (lower panel) the distribution shifts such that the Americas have the most events followed by the maritime continent and then Europe/Africa. This trend also occurs in higher LD-levels. The variance in longitudinal distribution may be due to regional differences in WWLLN detection efficiency as shown by Hutchins et al. [2012].

4.2 Geographic distribution of event/stroke pairs

The events are organized into 5-degree bins of latitude and longitude (Figure 2) using WWLLN stroke locations as the point of origin. We confirm that when all of these events are plotted the three “chimneys” of lightning activity are clearly visible over the Americas, Africa, and maritime continent (Figures 2 and 3).

The events with stroke location are further organized into large geographic groups of land, ocean, and coast. We define any of the original 5-degree bins neither fully land nor ocean to be coast- including the Hawaiian Islands and Fiji. The maritime continent additionally consists of many islands that are considered to be coast so we will compare just land and ocean.

The raw number of events with stroke location originating over the ocean is always greater than the number over the land (Table 2, Figure 4). We compare the fraction of events with stroke location that occur at each LD-level for both land and ocean (Figure 5). At higher LD-levels (LD 4 through LD 6), a greater fraction of events occur over the ocean than over the land. This indicates a greater probability for an over ocean stroke to register at a higher LD-level than a land stroke.

It is worthwhile to point out that this study only investigates events that correspond to strokes that fall within the inner FOV. All strokes that occurred outside the inner FOV were ignored. To justify ignoring strokes outside the inner FOV we selected a subset of events that occurred simultaneously with strokes exclusively in the inner FOV (discarding any events that occurred simultaneously with any stroke in the outer FOV). This yielded 4589 events with exclusively inner FOV strokes. The distribution of these events by LD-level for both ocean and land (Figure 6) is similar to the distribution of all inner events (Figure 4). Similarly, the fraction of total at each LD-level for the exclusively inner events (Figure 7) shows that a higher percentage of ocean strokes occur at LD 4 through LD 6 than land strokes.

5. Comparison to outgoing longwave radiation flux

A difference in physical lightning properties such as flash rate and radiance between land and ocean was reported by Boccippio et al [2000]. In section 4.2 we detail similar results that show a difference in optical power between land and ocean lightning. Analyses of the LD observations indicate that lightning with a high optical power occurs more frequently over the ocean than over the land. Suggested causes for this variance are cloud optical properties and water content [Boccippio et al., 2000].

We investigate one possible cause of such a difference in optical lightning power by comparing outgoing longwave radiation (OLR) fluxes at the top of the atmosphere (TOA). OLR values are influenced by cloudiness, cloud top temperature, and water vapor content. OLR values may be used as a proxy for convective activity [Waliser et al., 1993]. Thick clouds with high, cold tops such as deep convective clouds have a greater effect on diminishing the OLR than thinner, lower clouds with a smaller temperature difference [Chen et al., 1999].

In this study, OLR values were compared with 1,364 events sampled during 2009. The data used are from the NOAA/ERSL PSD data set where OLR values are determined from the hourly mean. Our initial analysis suggests that higher LD-levels correspond to an increased probability of low OLR (Figure 8). That is to say higher optical power events are statistically associated with strong convection.

Similar to the grouping method used in the previous section, an event was considered to be coast if it fell within 1 degree of either land or ocean. OLR values in land and ocean groups were then averaged (Table 4). The land group proved to have a lower average OLR value than the ocean group which is consistent with more convective clouds occurring over land. We conclude that OLR alone is not capable of identifying difference in cloud properties that may be responsible for the underlying differences in oceanic versus land-based lightning.

6. Synthesis

Our preliminary assessment of the LD instrument aboard the C/NOFS satellite in conjunction with WWLLN confirms three dense lightning chimneys- Central and South America, Congo Basin, and the Maritime Continent. First we conducted a comparison of C/NOFS events of a given LD-level and found the number of events with stroke location to be lower than expected over Africa when compared to the

total number of events observed by the LD. Secondly, a greater number of high powered optical emissions were detected over the ocean than land. This finding is consistent with previous work by Boccippio et al. [2000]. Finally, we compared outgoing longwave radiation fluxes at the top of the atmosphere in North America with events to determine if OLR may contribute to the difference between land and ocean lighting emissions. We found that higher LD-level events generally originate in low OLR flux regions suggesting that high optical power events are statistically associated with strong convection. Additionally, the mean OLR value for all accumulated land events is statistically lower than that of ocean events. We advocate that further studies are needed to address the cause for physical differences between land and ocean lightning emissions.

References

Abarca et al., 2010: An evaluation of the Worldwide Lightning Location Network (WWLLN) using the National Lightning Detection Network (NLDN) as ground truth.

Boccippio et al, 2000: Regional differences in tropical lightning distributions. *J. Appl. Meteor*. 39, 2231-2248.

Chen et al., 2000: Radiative effects of cloud-type variations. *Journal of Climate*

Dowden et al., 2002: VLF lightning location by time of group arrival (TOGA) at multiple sites. *Journal of Atmospheric and Solar-Terrestrial Physics*

Gatlin and Goodman, 2010: Preliminary Development and Evaluation of Lightning Jump Algorithms for the Real-Time Detection of Severe Weather. *J. Appl. Meteor. Climatol.*

Heddinghaus, T. R. and A. F. Krueger, 1981: Annual and Interannual Variations in Outgoing Longwave Radiation over the Tropics. *Monthly Weather Review*, 109, 1208

Hsu et al., 2009: On the global occurrence and impacts of transient luminous events (TLEs). *AIP Conference Proceedings.*

Hutchins et al., 2012 Far-field power of lightning strokes as measured by the world wide lightning location network. *Journal of Atmospheric and Oceanic Technology.*

Jacobson et al. 2011: Initial studies with the Lightning Detector on the C/NOFS satellite, and cross-validation with WWLLN.

Lay et al. 2004: WWLL global lightning detection system: Regional validation study in Brazil. *Geophysical Research Letters*

Lay et al., 2007 Time Variation in Land/Ocean Lightning Count Rates as Measured by the World Wide Lightning Location Network, *J. Geophys. Res*

MacGorman et al., 1989: Lightning rates relative to tornadic storm evolution on 22 May 1981. *J. Atmos.* Sci.,28, 221-250.

Mesinger, Fedor et. Al., 2004: North American Regional Reanalysis: A long-term, consistent, high-resolution climate dataset for the North American domain, as a major improvement upon the earlier global reanalysis datasets in both resolution and accuracy. *Bulletin of the American Meteorological Society.*

Orville, R.E. and W. Henderson, 1986: Global distribution of midnight lightning: September 1977 to August 1978. *Mon. Wea. Rev.,* 114, 2640-2653.

Price, C, and D. Rind 1992: A Simple Lightning Parameterization for Calculating Global Lightning Distributions. *J. Geo. Rev*., 97, 9919–9933.

Rodger et al., 2003: Significance of lightning generated whistlers to inner radiation belt electron lifetimes. *Journal of Geophysical Research*

Rodger et al., 2005: Location accuracy of VLF World-Wide Lightning Location (WWLL) network: Post-algorithm upgrade. *Annales Geophysicae*

Sabbas et al., 2010: The behavior of total lightning activity in severe Florida thunderstorms. *Atmospheric Research*

Ushio et al., 2001: A survey of thunderstorm flash rates compared to cloud top height using TRMM satellite data. *Journal of Geophysical Research,* 106, 24089.

Waliser et al., 1993: Comparison of the Highly Reflective Cloud and Outgoing Longwave Radiation Datasets for Use in Estimating Tropical Deep Convection. *Journal of Climate*

Williams et al., 1999: The behavior of total lightning activity in severe Florida thunderstorms. *Atmospheric Research*

Zajac, B. A., and Rutledge, S. A., 2001: Cloud-to-Ground Lightning Activity in the Contiguous United States from 1995 to 1999. *American Meteorological Society*.

Figures and Tables

	LD 0	LD 1	LD 2	LD 3	LD 4	LD 5	LD 6
Raw	19604	929	186	49	17	3	1
Altitude correction	6443	7342	3038	1957	1109	333	567

Table 1: The raw versus altitude corrected number of event with stroke location.

LD-level	Land	Ocean
LD 0	1583 +/- 78.01	1928 +/- 86.08
LD 1	1651 +/- 79.66	2358 +/- 1-5.28
LD 2	776 +/- 54.63	884 +/- 59
LD 3	489 +/- 43.39	600 +/- 48.1
LD 4	197 +/- 27.58	444 +/- 41.35
LD 5	42 +/- 12.86	128 +/- 22.26
LD 6	99 +/- 19.6	187 +/- 26.87

Table 2: The distribution of events with stroke locations by LD-level for land and ocean. The confidence interval is given in parenthesis using Poisson statistics: (1+/-(1.96/sqrt(N-1)))N

	Land	Ocean
Average OLR value	169.2 (1.6)	248.8 (1.4)

Table 3: Average outgoing longwave radiation flux (OLR) at the top of the atmosphere for land and ocean. Uncertainty (determined by the standard deviation over the square root of the number of samples) is given in parentheses.

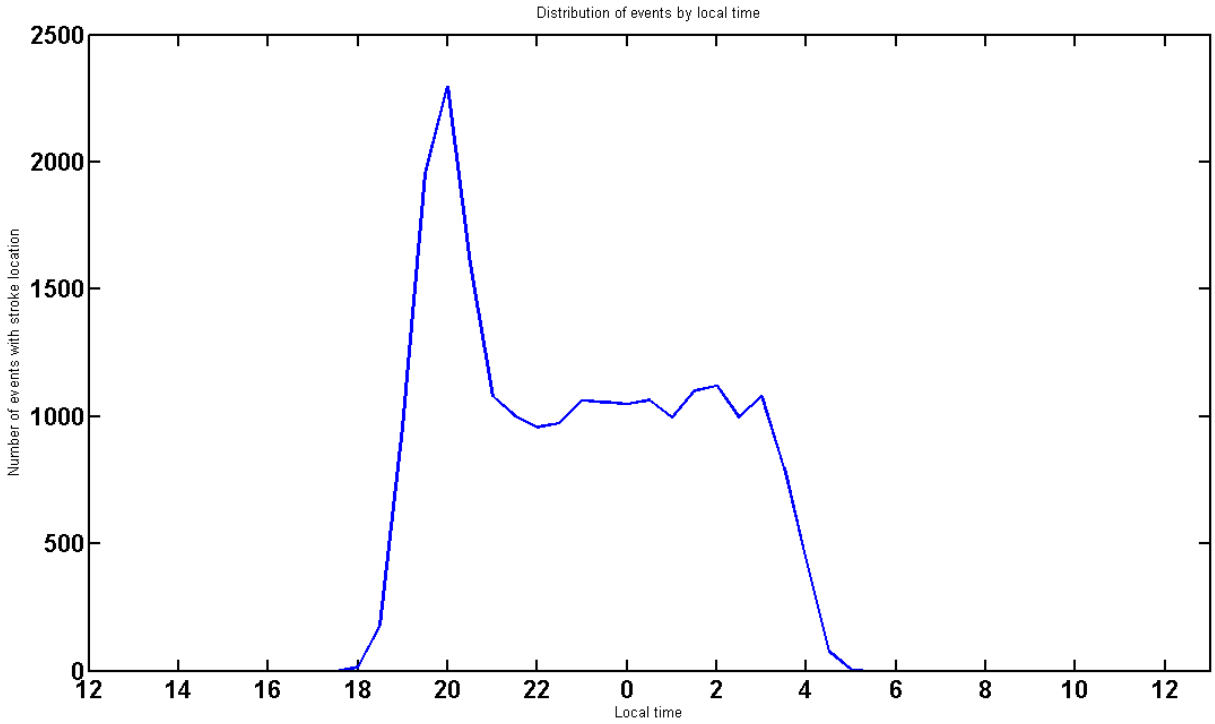

Figure 1: Temporal distribution of events with stroke location. The number of events peaks at 2000 local time and no events occur during the period between 0500 and 1800.

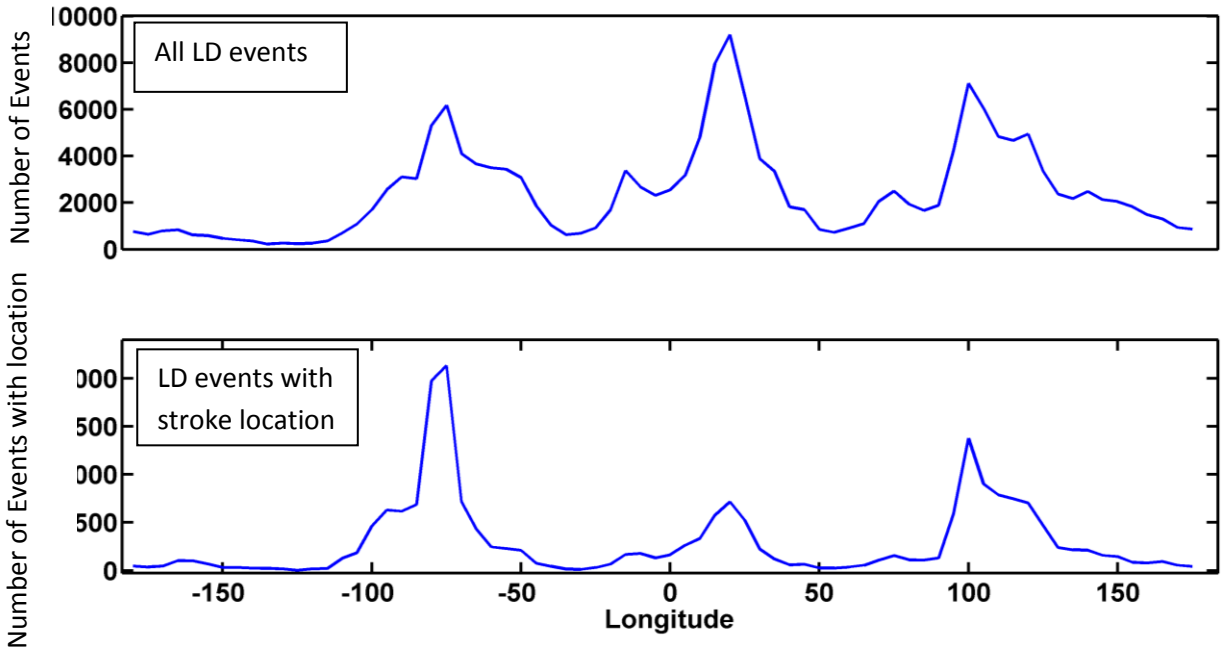

Figure 2: Comparison of all LD optical emission detections of LD 0 or greater (top) and events LD 0 or greater with stroke location (bottom).

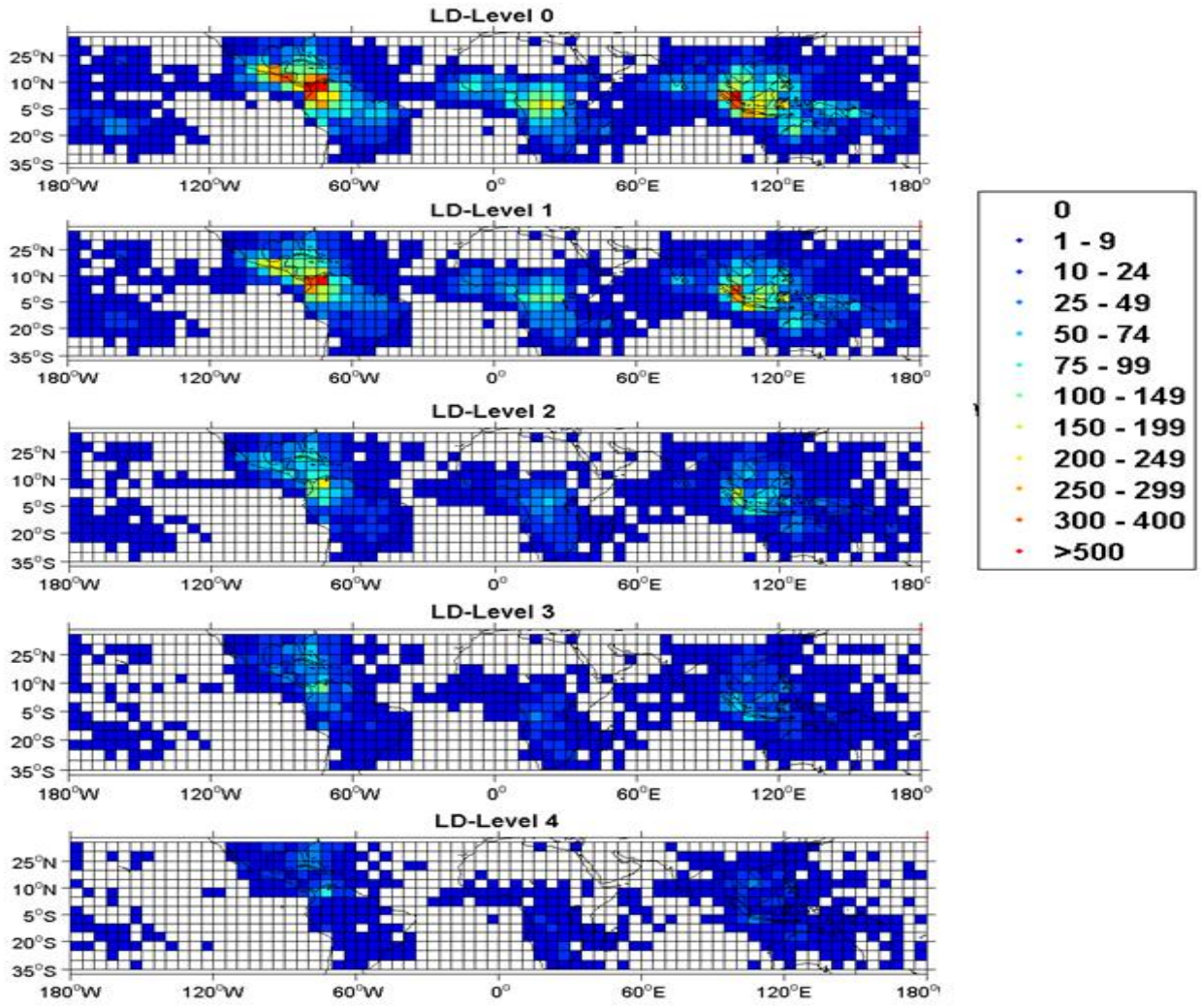

Figure 3: Showing the geographical distribution of altitude corrected events registering at LD 0 or higher through LD 4 and higher.

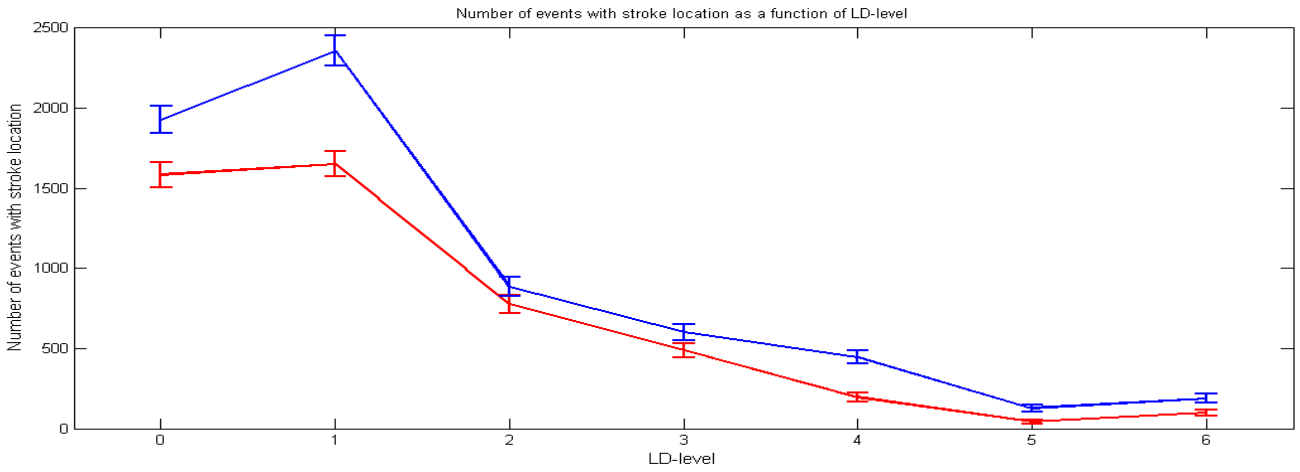

Figure 4: Number of events by LD-level. Uncertainty is determined using Poisson statistics (1+/-(1.96/sqrt(N-1)))N.

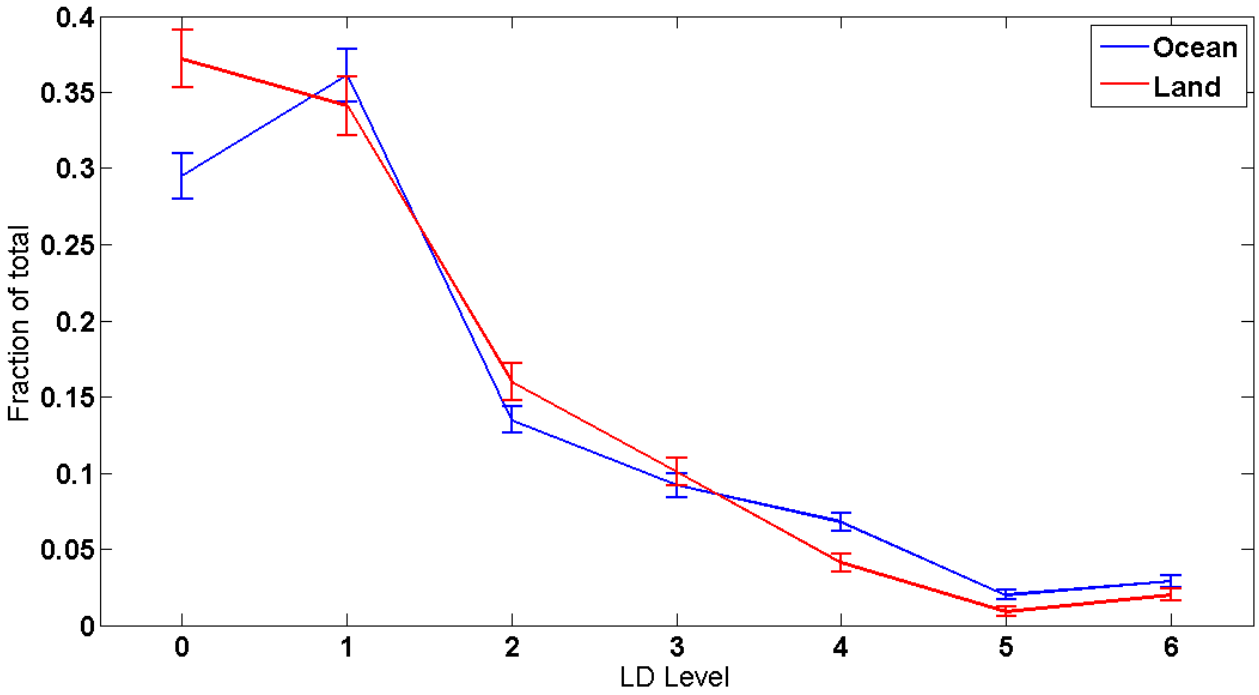

Figure 5: Fraction of total events at each LD-level for both ocean and land. Uncertainty is determined using Poisson statistics.

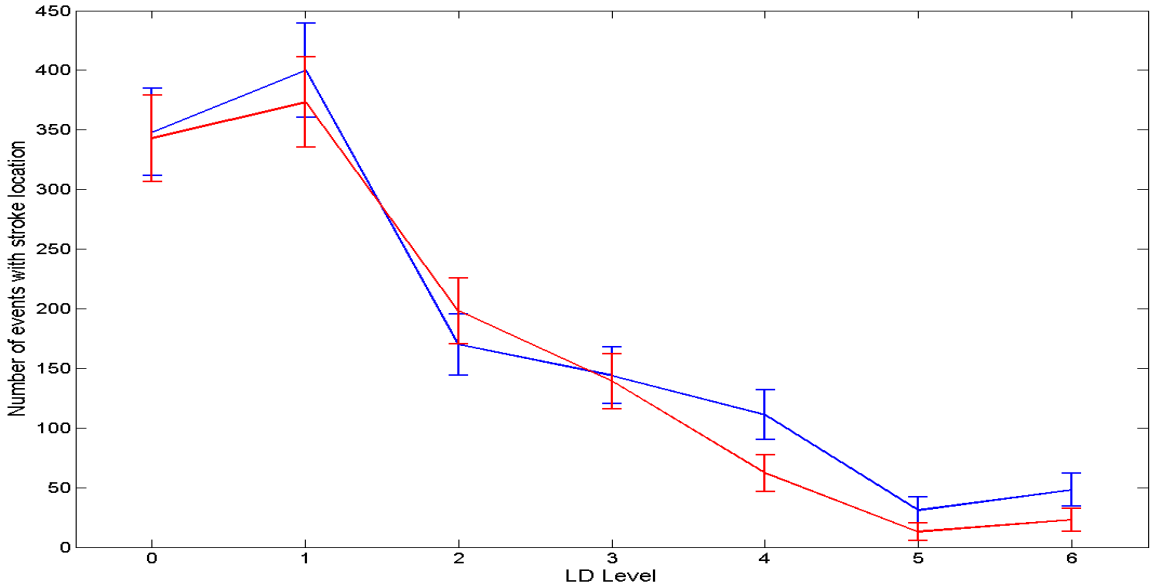

Figure 6: Distribution of exclusively inner events by LD-level. Compare to Figure 4. Uncertainty determined by Poisson statistics.

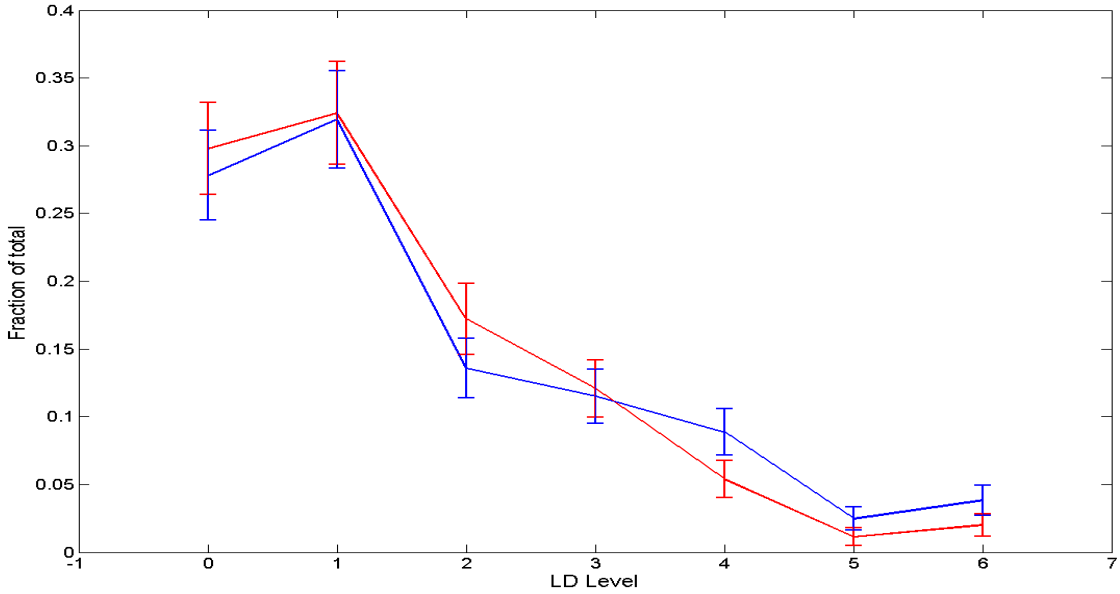

Figure 7: Fraction of total exclusively inner events. Compare to Figure 5. Uncertainty determined by Poisson statistics.

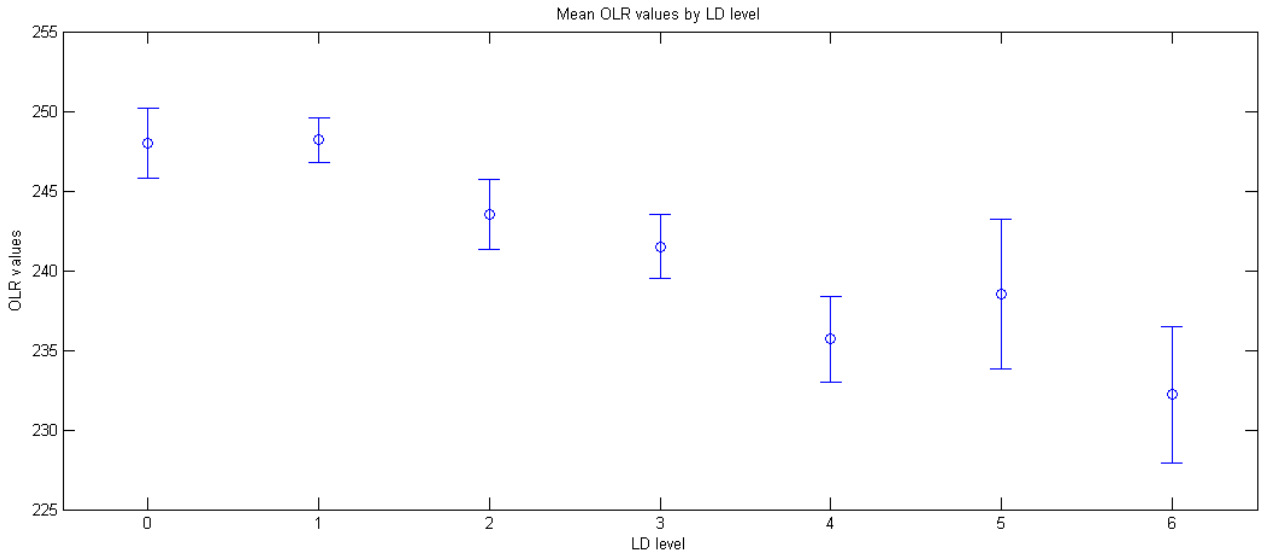

Figure 8: Mean OLR values for all event pairs by LD-level. Uncertainty is shown using standard error σ/sqrt(N).